Journal of Nuclear Cardiology (xxxx) xxx, xxx

ORIGINAL RESEARCH

Stenosis degree and plaque burden differ between the major epicardial coronary arteries supplying ischemic territories

Tanja Kero, MD, PhD [1,2,*], Juhani Knuuti, MD, PhD [2,3,7], Sarah Bär, MD, PhD [2,4], Jeroen J. Bax, MD, PhD [5], Antti Saraste, MD, PhD, FESC [2,6], Teemu Maaniitty, MD, PhD [2,7]

[1] Nuclear Medicine & PET, Department of Surgical Sciences, Uppsala University, Uppsala, Sweden
[2] Turku PET Centre, Turku University Hospital and University of Turku, Turku, Finland
[3] InFlames Flagship, University of Turku, Turku, Finland
[4] Department of Cardiology, Bern University Hospital Inselspital, Bern, Switzerland
[5] Department of Cardiology, Leiden University Medical Center, Leiden, the Netherlands
[6] Heart Center, Turku University Hospital, University of Turku, Turku, Finland
[7] Department of Clinical Physiology, Nuclear Medicine, and PET, Turku University Hospital, Turku, Finland

[*] Corresponding author. PET Center / Medical Imaging Center, Uppsala University Hospital, 75185 Uppsala, Sweden.
E-mail address: tanja.kero@uu.se (Tanja Kero).

Abstract

Background: It is unclear whether coronary artery stenosis, plaque burden, and composition differ between major epicardial arteries supplying ischemic myocardial territories.

Methods: We studied 837 symptomatic patients undergoing coronary computed tomography angiography (CTA) and ^{15}O-water positron emission tomography (PET) myocardial perfusion imaging for suspected obstructive coronary artery disease. Coronary CTA was analyzed using artificial intelligence-guided quantitative computed tomography (AI-QCT) to assess stenosis and atherosclerotic plaque characteristics. Myocardial ischemia was defined by regional PET perfusion in the left anterior descending (LAD), left circumflex (LCX), and right coronary artery (RCA) territories.

Results: Among arteries supplying ischemic territories, the LAD exhibited significantly higher stenosis and both absolute and normalized plaque volumes compared to LCX and RCA ($P < .001$ for all). Multivariable logistic regression showed diameter stenosis ($P = .001$-$.015$), percent atheroma volume (PAV; $P < .001$), and percent noncalcified plaque volume (NCPV) ($P = .001$-$.017$) were associated with ischemia across all three arteries. Percent calcified plaque volume (CPV) was associated with ischemia only in the RCA ($P = .001$).

Conclusions: The degree of stenosis and atherosclerotic burden are significantly higher in the LAD as compared to LCX and RCA, both in epicardial coronary arteries supplying nonischemic or ischemic myocardial territories. In all the three main coronary arteries, both luminal narrowing and plaque burden are independent predictors of ischemia, where the plaque burden is mainly driven by noncalcified plaque. However, many vessels supplying ischemic territories have a relatively low degree of stenosis and plaque burden, especially in the LCX and RCA, limiting the ability of diameter stenosis and PAV to predict myocardial ischemia.

Keywords: Coronary computed tomography angiography, Artificial intelligence, Coronary plaque, Ischemia, Positron emission tomography

Received 6 April 2025; Accepted 29 July 2025; Available online XXX

https://doi.org/10.1016/j.nuclcard.2025.102470

ABBREVIATIONS

CAD	coronary artery disease
CTA	computed tomography angiography
PET	positron emission tomography
AI-QCT	artificial intelligence-guided quantitative computed tomography
PAV	percent atheroma volume
CPV	percent calcified plaque volume
NCPV	percent noncalcified plaque volume
LAPV	percent low-attenuation plaque volume
MBF	myocardial blood flow
FFR	fractional flow reserve

INTRODUCTION

Coronary computed tomography angiography (CTA) has, over recent years, become the first-line test for suspected coronary artery disease (CAD) in patients with a moderate or low pretest clinical likelihood of CAD [1]. Coronary CTA allows for assessment of atherosclerotic plaque quantity and composition (calcified, noncalcified, low density) and high-risk plaque characteristics that are known to have diagnostic and prognostic information [2]. Emerging evidence also suggests a relationship between plaque features and ischemia in patients with CAD [3–5]. Plaque burden and phenotype also appear to differ between the major coronary arteries [6]. However, little information is available about the vessel-specific relationship between coronary artery plaque burden and composition and myocardial ischemia.

Recently, application of artificial intelligence to the analysis of coronary CTA has enabled rapid, objective, and reproducible quantification of coronary artery stenosis and plaque volumes [7–9]. Artificial intelligence-guided quantitative computed tomography (AI-QCT) is a novel, Food and Drug Administration (FDA)-cleared coronary stenosis and plaque characterization and quantification tool [7,8].

In a recent study we found that the addition of AI-QCT quantitative measures of percent atheroma volume and noncalcified plaque volume (NCPV) to clinical variables and degree of stenosis improved the detection of ischemic CAD on a patient level [10]. Our hypothesis is that coronary artery plaque burden and morphology, in addition to luminal narrowing, would contribute to myocardial ischemia at a regional level and might vary in the main epicardial coronary arteries. Therefore, in this study, we assessed and compared the atherosclerotic plaque burden and phenotype of the major epicardial coronary arteries supplying ischemic myocardial territories in symptomatic patients with suspected obstructive CAD.

METHODS

Patients

The study population was derived from the Turku cardiac CTA registry at the Turku University Hospital, Finland. The registry includes symptomatic patients who underwent coronary CTA for suspected CAD from February 2007 to December 2016. Patients with previously known obstructive CAD, myocardial infarction (MI), percutaneous coronary intervention (PCI), or coronary artery bypass grafting (CABG) were not considered for inclusion.

According to the institutional imaging protocol, patients with suspected CAD first undergo coronary CTA. If the CTA reveals at least one suspected obstructive or clearly obstructive coronary artery stenosis (using visual $\geq$50% diameter stenosis as a guideline), the patient is referred for downstream stress ^{15}O-water positron emission tomography (PET) myocardial perfusion imaging (MPI) for hemodynamic assessment of the stenosis. For patients without visual obstructive stenosis, additional imaging is not required. This selective functional testing is supported by the current guidelines [1]. Demographic data, cardiovascular risk factors, and symptoms were retrospectively collected from the medical records of Turku University Hospital.

The study complies with the Declaration of Helsinki. The Ethics Committee of the Hospital District of Southwest Finland approved the study protocol and waived the need for written informed consent.

Coronary CTA and PET imaging procedures

Coronary CTA scans were performed with 64-row hybrid PET-CT scanners (GE Discovery VCT or GE D690, General Electric Medical Systems, Waukesha, USA) as previously described [11]. Before coronary CTA image acquisition, intravenous metoprolol (0-30 mg) to achieve a target heart rate of 60 bpm and oral/sublingual nitrate were administered. Coronary CTA was performed using intravenously administered low-osmolal iodine contrast agent. Prospectively triggered acquisition was applied whenever feasible.

Based on the initial visual evaluation of the coronary CTA findings, patients with suspected obstructive stenosis on CTA underwent dynamic quantitative PET perfusion scan during adenosine stress using a hybrid PET-CT scanner, usually in the same imaging session [11,12]. ^{15}O-labeled water ([^{15}O]H_2O) was used as a radiotracer, and adenosine infusion (140 μg/kg/min) was used for vasodilator stress. The patients were instructed to abstain from caffeine for 24 hours before the PET study. In some patients, perfusion imaging was performed in the following days or weeks due to logistic reasons or caffeine use.

AI-QCT analysis

Visual coronary CTA reading was used in clinical practice to guide downstream PET referral. For research purposes, coronary CTA scans were reanalyzed in 2022-2023 in a blinded manner using a previously described AI-QCT algorithm (Cleerly LABS, Cleerly Inc., Denver, CO, USA) [7,8]. This commercially available FDA-cleared software utilizes a series of validated convolutional neural networks (3D U-Net and VGG network variants) for image quality assessment, coronary artery segmentation and labeling, lumen wall evaluation and vessel contour determination, and plaque characterization.

The AI-QCT allows for assessing coronary artery lesions where plaque is present. Utilizing a normal proximal reference vessel cross-sectional slice, the start and the end of the lesion, and the cross-sectional slice that demonstrates the greatest absolute narrowing, the % diameter stenosis severity was automatically calculated. Remodeling index (RI) was calculated as the outer vessel diameter/the mean of the diameter of the normal adjoining segments, and positive remodeling was defined as RI $>$ 1.1 [14]. Within coronary artery lesions, plaque volume was quantified and further characterized as low-attenuation plaque, noncalcified plaque, and calcified plaque based upon Hounsfield unit (HU) densities $<$30, 30 to 350, $>$350, respectively [7]. Vessel volumes, lumen volumes, plaque volumes, diameter and area stenosis, and remodeling index were recorded for each major coronary artery including their side branches ($>$1.5 mm in diameter). Plaque volumes (mm^3) were calculated for each coronary lesion and then summed to compute the total plaque volumes in the left main (LM), left anterior descending (LAD), left circumflex (LCX) and right coronary artery (RCA). For each vessel, the sum of plaque volumes of all lesions was divided by the vessel volume to obtain the total plaque burden, reported as percent atheroma volume (PAV, %) and its components: percent calcified plaque volume (CPV, %) and percent NCPV. Due to small quantities, low-attenuation plaque volume (LAPV) was pooled together with NCPVs into NCPV and was also separately reported as a binary variable (presence/absence of low-attenuation plaque). The most severe stenosis degree and the highest RI were reported for each major coronary artery. Variables from the LM artery were integrated in both the LAD and LCX artery analyses. Specifically, vessel, lumen, and plaque volumes of LM were added to plaque volumes of both LAD and LCX, whereas maximal stenosis degree and remodeling index were assigned to both LAD and LCX in case they were observed in the LM. This approach was chosen to reflect the contribution of LM atherosclerosis and stenosis to downstream perfusion in both daughter vessels.

PET analysis

The PET perfusion data were quantitatively analyzed using Carimas software (developed at Turku PET Centre, Turku, Finland) in standardized 17 segments according to the American Heart Association, and individual myocardial segments were assigned to the three major coronary arteries as recommended [15]. Hyperemic myocardial blood flow (MBF), expressed in mL $min^{-1}g^{-1}$ of perfusable myocardial tissue, was calculated for the standardized 17 segments. The presence of myocardial ischemia was defined as hyperemic MBF $\leq$2.30 mL $min^{-1}g^{-1}$ in at least two adjacent segments, excluding the basal septum [16]. Regional hyperemic MBF was calculated as the mean of two adjacent segments with the lowest perfusion within a coronary artery territory.

Vessel dominance was defined based on which vessel the posterior descending artery (PDA) originated from on coronary CTA. For right dominance, the PDA originated from the RCA, for left dominance, the PDA originated from the LCX, and for codominance, there were PDA branches from both the RCA and LCX. In right dominant and codominant cases, the inferoseptal and inferior myocardial segments were assumed to be perfused by the RCA and assigned to RCA myocardial territory, whereas in left dominant cases the inferoseptal and inferior myocardial segments were assumed to be perfused by the LCX and were included in the LCX myocardial territory.

Statistical analysis

Continuous variables are shown as mean ± SD or median (interquartile range [25th-75th percentile]). Categorical variables are shown as numbers

with percentages. The Shapiro–Wilk test was used to assess the normality of the data distribution.

The Mann–Whitney *U* test and Kruskal–Wallis test were used to compare continuous variables. The Chi-square test was used for categorical variables. Different coronary arteries (LAD, LCX, RCA) were considered independent samples. For pairwise comparisons, the significance values were adjusted by the Dunn's or the Bonferroni correction for multiple tests. Logistic regression was used to determine AI-QCT variables associated with myocardial ischemia. Variables with a significant association in univariable analysis were included in the multivariable models. Combinations of variables that would lead to collinearity were avoided and tested using the variance inflation factor (VIF). The predicted probability of ischemia as a function of diameter stenosis or PAV was derived from univariable binary logistic regression for each major coronary artery separately, and depicted as sigmoid curves. The points where the probability of ischemia equals to .5 were estimated for each coronary artery and compared between vessels using a Z-test.

To evaluate and compare the performance of the AI-QCT variables in the prediction of ischemia, the areas under the receiver operating characteristic curves (AUCs) were calculated and compared using the method by DeLong for dependent samples and [17] the method by Hanley and McNeil for independent samples [18,19].

Analyses were two-tailed and a *P*-value of $<.05$ was considered statistically significant. Statistical analyses were performed using IBM SPSS statistics for Macintosh (Version 29.0.2.0 Armonk, NY: IBM Corp), GraphPad Prism (version 10, GraphPad Software, La Jolla California), R version 4.3.2, and VassarStats: Website for Statistical Computation (vassarstats.net).

RESULTS

Study cohort

Out of the 2411 consecutive symptomatic patients with coronary CTA, 837 (35%) patients underwent downstream PET MPI according to the institutional selective hybrid imaging protocol, and had coronary CTA quantitatively analyzed by AI-QCT (Figure 1). Out of the 837 patients who underwent PET MPI, the most severe diameter stenosis per patient was a median of 50 (28-66%,) and 360 (43%) had myocardial ischemia based on the presence of abnormal regional stress perfusion on a patient level (130 [29%] with single-vessel, 120 [33%] with two-vessel, and 137 [38%] with three-vessel ischemia). Right vessel dominance was present in 703 (84%), left vessel dominance in 84 (10%), and codominance in 50 (6%) patients. On a vessel level, ischemia was present in 279 (33%) of the LAD territories, 213 (25%) of the LCX territories, and 212 (28%) of the RCA territories ($P < .001$). Among ischemic myocardial territories, regional hyperemic MBF was a median interquartile range of 1.61 (1.19-1.90) mL $min^{-1}g^{-1}$ in the LAD, 1.65 (1.26-1.93) mL $min^{-1}g^{-1}$ in the LCX, and 1.50 (1.13-1.79) mL $min^{-1}g^{-1}$ in the RCA territories ($P < .001$) and the

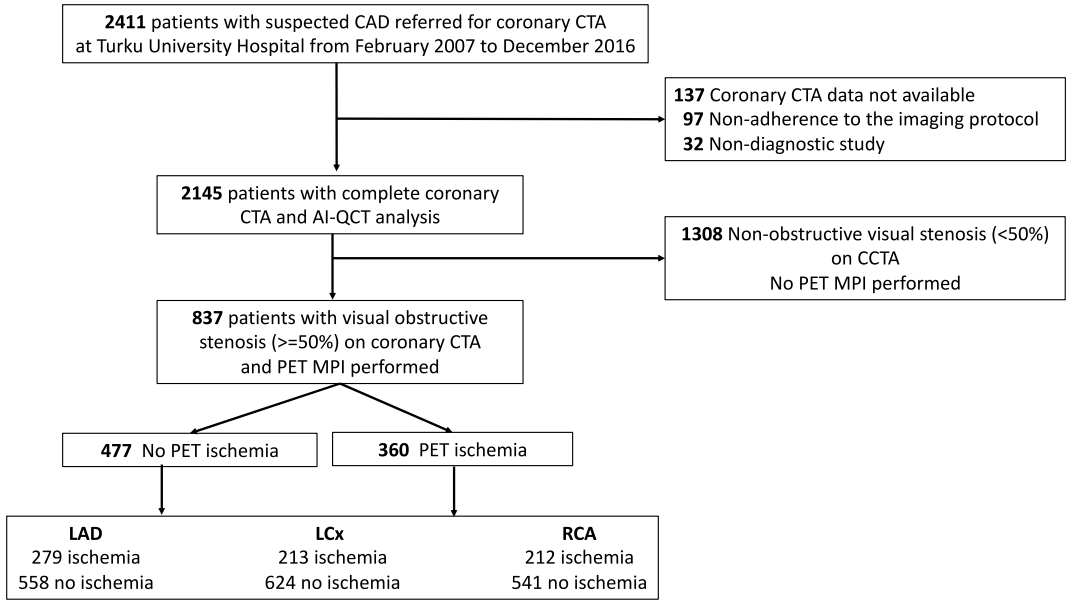

Figure 1. Patient flowchart. CAD = coronary artery disease, CTA = computed tomography angiography, AI-QCT = artificial intelligence-guided quantitative computed tomography, PET = positron emission computed tomography, LAD = left anterior descending coronary artery, LCx = left circumflex coronary artery, RCA = right coronary artery.

number of ischemic segments (hyperemic MBF $\leq$2.30 mL $min^{-1}g^{-1}$) was a median interquartile range of 5 (3-6) in the LAD, 5 (3-5) in the LCX, and 4 (3-4) in the RCA territories ($P < .001$).

The clinical characteristics of the patients are shown in Table 1.

Stenosis degree and plaque features in main epicardial coronary arteries

The AI-QCT analysis variables of vessel and plaque features for each main coronary artery are summarized in Table 2. The stenosis degree and the plaque burden were generally higher in the LAD than in the LCX and RCA. Variables from the LM artery were incorporated into both the LAD and LCX vessel-level analyses to reflect its contribution to downstream perfusion. In the study population, LM plaque burden was generally low, with a median diameter stenosis of 7% (IQR: 0-19), total plaque volume of 15.7 mm^3 (1.5-43.3), NCPV 10.1 mm^3 (1.0-25.4) and CPV 1.4 mm^3 (.0-15.4).

Comparison of vessel and plaque features from vessels supplying ischemic vs nonischemic myocardial territories is summarized in Table 3. As expected, stenosis degree, remodeling index, and all plaque measures were higher in the vessels supplying ischemic territories compared to the vessels supplying nonischemic territories. Figures 2 and 3 show the distribution of diameter stenosis and PAV in vessels supplying ischemic and nonischemic territories.

A comparison of vessel and plaque measures from the coronary arteries that supply the ischemic territories is shown separately in Table 4. Among the epicardial coronary arteries supplying ischemic territories, the degree of stenosis was highest in the LAD, followed by the RCA, and lowest in the LCX (all pairwise comparisons statistically significant). Absolute and normalized plaque volumes and their components were higher in the LAD compared to the other main coronary arteries. In addition, RCA had higher total and NCPVs compared to the LCX in absolute terms, but these were not statistically significant when the size of the vessel was taken

Table 1. Patient characteristics

Patient characteristics	N = 837
Age, years	65 [59-71]
Sex (male), n (%)	441 (52.7%)
Hypertension, n (%)	552 (65.9%)
Dyslipidemia, n (%)	594 (71.0%)
Current/previous smoker, n (%)	328 (39.2%)
Diabetes mellitus, n (%)	156 (18.6%)
Family history of CAD, n (%)	394 (47.1%)
Typical angina, n (%)	243 (29.0%)
BMI, kg/m^2	27.3 [24.7-30.5]
Agatston coronary artery calcium score	249 [43-671]
Antiplatelet drug, n (%)	445 (53.2%)
Lipid-lowering drug, n (%)	421 (50.3%)
Beta-blocker, n (%)	438 (52.3%)
Long-acting nitrate, n (%)	92 (11.0%)
Calcium channel blocker, n (%)	166 (19.8%)
ACE inhibitor, n (%)	175 (20.9%)
AT II antagonist, n (%)	197 (23.5%)

Values are n (%) or median [interquartile range]. *CAD*, coronary artery disease; *BMI*, body mass index; *ACE*, angiotensin converting enzyme, *AT II*, angiotensin II.

Table 2. Characteristics of the main coronary arteries by AI-QCT analysis of coronary computed tomography angiography

	LAD	LCX	RCA	P-value	P-value LAD vs LCX	P-value LAD vs RCA	P-value LCX vs RCA
Vessel volume, mm^3	1151 [907-1455]	861 [625-1163]	1186 [821-1584]	<.001	<.001	1.000	<.001
Lumen volume, mm^3	947 [755-1196]	776 [541-1041]	1029 [697-1402]	<.001	<.001	.085	<.001
Remodeling index	1.3 [1.2-1.5]	1.3 [1.2-1.4]	1.2 [1.1-1.4]	<.001	<.001	<.001	.039
Diameter stenosis, %	42 [23-59]	19 [8-34]	21 [7-45]	<.001	<.001	<.001	.008
Area stenosis, %	67 [40-84]	34 [14-57]	37 [11-69]	<.001	<.001	<.001	.022
Total plaque volume, mm^3	159 [69-291]	58 [19-135]	69 [15-190]	<.001	<.001	<.001	.045
NCPV, mm^3	92 [43-154]	39 [15-80]	45 [14-121]	<.001	<.001	<.001	<.001
CPV, mm^3	52 [12-126]	13 [.4-54]	11 [.0-60]	<.001	<.001	<.001	.868
Percent PAV, %	14 [7-23]	7 [2-15]	6 [2-16]	<.001	<.001	<.001	.728
Percent NCPV, %	8 [4-12]	5 [2-9]	4 [1-10]	<.001	<.001	<.001	1.000
Percent CPV, %	5 [1-11]	2 [0-6]	1 [0-5]	<.001	<.001	<.001	.011
Low attenuation plaque, %	245 (29)	124 (15)	157 (19)	<.001	<.001	<.001	.11

Values are n (%) or median [interquartile range]. *AI-QCT*, artificial intelligence-guided quantitative computed tomography; *LAD*, left descending artery; *LCX*, left circumflex artery; *RCA*, right coronary artery; *NCPV*, non-calcified plaque volume; *CPV*, calcified plaque volume. For pairwise comparisons, *P*-values were adjusted using the the Dunn's correction for multiple tests or Bonferroni correction to control for multiple comparisons.

Table 3. Comparison of AI-QCT characteristics of coronary arteries supplying ischemic and non-ischemic myocardial territories

	LAD			LCX			RCA		
	Ischemic	Nonischemic	P-value	Ischemic	Nonischemic	P-value	Ischemic	Nonischemic	P-value
Vessel volume, mm^3	1216 [954-1501]	1134 [881-1398]	.007	963 [638-1291]	847 [624-1123]	.018	1210 [930-1591]	1259 [920-1649]	.426
Lumen volume, mm^3	927 [744-1142]	968 [761-1225]	.047	790 [497-1099]	770 [545-1024]	.954	985 [685-1303]	1172 [849-1528]	<.001
Remodeling index	1.4 [1.3-1.6]	1.3 [1.2-1.4]	<.001	1.4 [1.2-1.5]	1.2 [1.1-1.4]	<.001	1.3 [1.2-1.5]	1.2 [1.1-1.3]	<.001
Diameter stenosis, %	55 [39-71]	34 [18-53]	<.001	31 [18-50]	16 [6-29]	<.001	45 [24-66]	17 [6-34]	<.001
Area stenosis, %	82 [62-92]	57 [32-78]	<.001	52 [32-75]	28 [10-49]	<.001	69 [40-89]	29 [9-56]	<.001
Total plaque volume, mm^3	241 [148-380]	126 [49-217]	<.001	125 [50-221]	45 [14-104]	<.001	176 [75-348]	50 [14-158]	<.001
NCPV, mm^3	128 [77-200]	68 [31-127]	<.001	67 [34-112]	31 [11-67]	<.001	106 [44-200]	38 [13-96]	<.001
CPV, mm^3	89 [31-197]	39 [8-101]	<.001	38 [10-104]	8 [0-35]	<.001	44 [8-137]	7 [0-47]	<.001
Percent atheroma volume, %	21 [13-31]	11 [5-18]	<.001	14 [6-24]	6 [2-12]	<.001	16 [7-27]	4 [1-11]	<.001
Percent NCPV, %	11 [7-16]	6 [3-10]	<.001	7 [4-13]	4 [1-7]	<.001	9 [6-16]	3 [1-8]	<.001
Percent CPV, %	8 [3-16]	4 [1-8]	<.001	4 [1-10]	1 [0-4]	<.001	4 [1-11]	.5 [0-3]	<.001
Presence of low attenuation plaque, n(%)	125 (45)	120 (22)	<.001	45 (21)	79 (13)	.003	73 (34)	76 (14)	<.001

Values are n (%) or median [interquartile range].
AI-QCT, artificial intelligence-guided quantitative computed tomography; *LAD*, left descending artery; *LCX*, left circumflex artery; *RCA*, right coronary artery; *NCPV*, non-calcified plaque volume; *CPV*, calcified plaque volume.

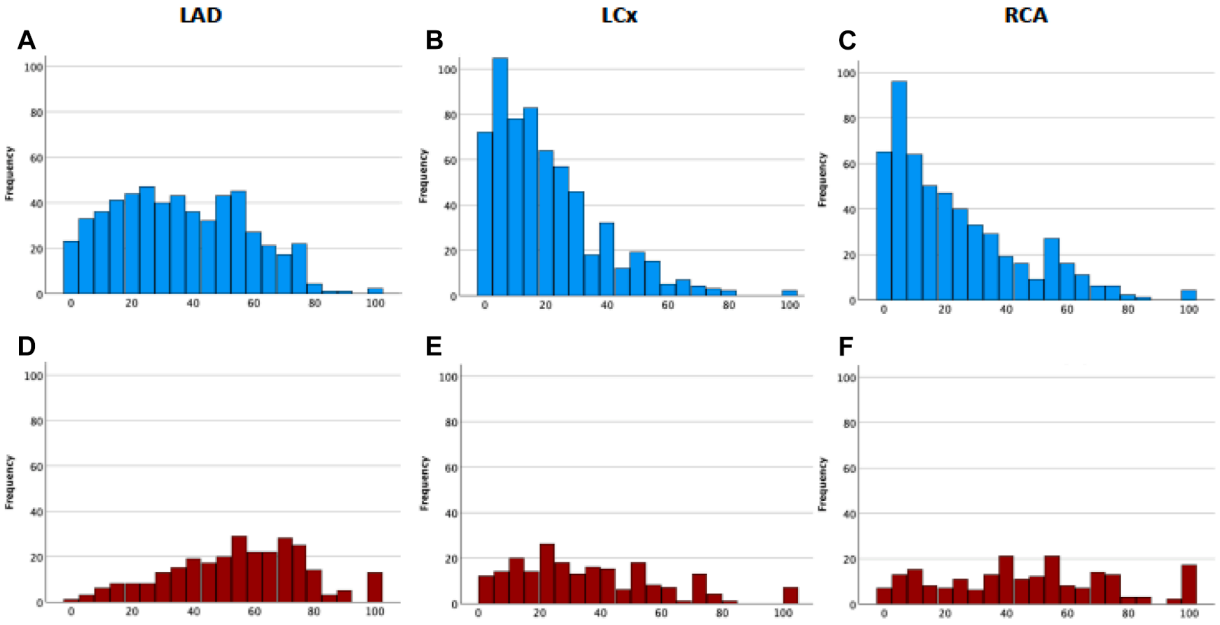

Figure 2. Histograms showing the distribution of diameter stenosis (%) in coronary arteries supplying nonischemic (A, B, and C; histogram bars in blue) and ischemic (D, E, and F; histogram bars in red) myocardial territories for LAD (A and D), LCX (B and E), and RCA (C and F). LAD, left anterior descending coronary artery, LCX, left circumflex coronary artery, RCA, right coronary artery.

into account. Interestingly, the presence of low-attenuation plaque was statistically higher in the LAD than the LCX, but not when compared to the RCA. Finally, the LAD had a higher remodeling index than the RCA and LCX, but it was not statistically different between the LCX and RCA.

Stenosis degree and plaque characteristics as predictors of ischemia

Results from univariable and multivariable logistic regression analyses to identify AI-QCT variables associated with myocardial ischemia in the three main coronary arteries separately are shown in Table 5. Stenosis degree, remodeling

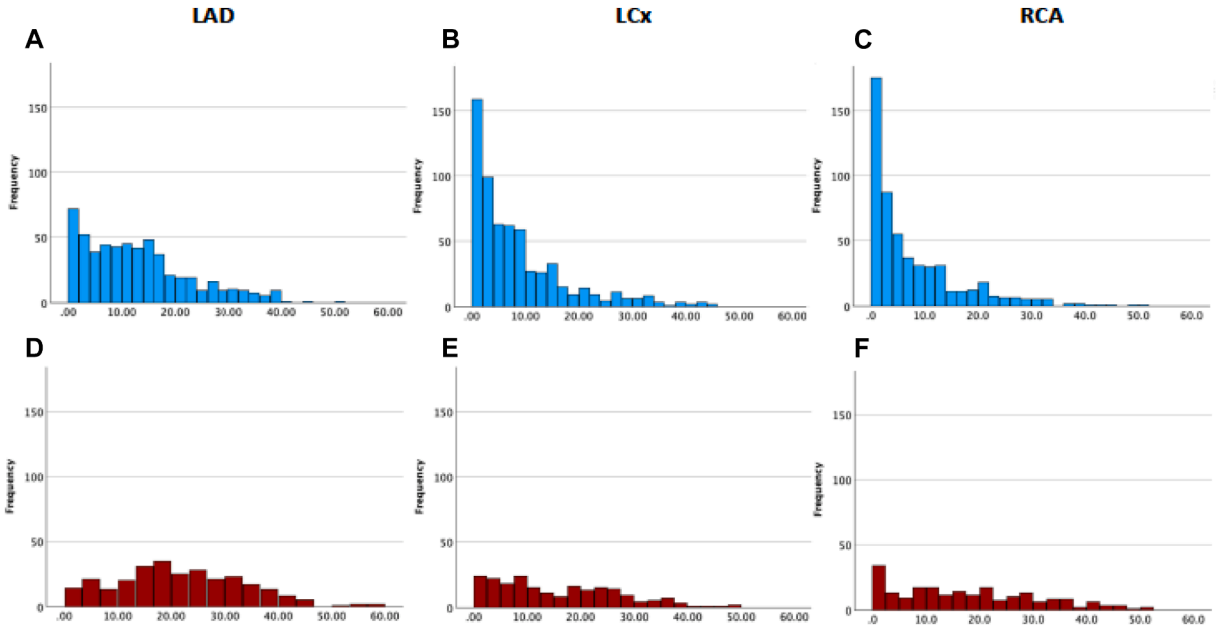

Figure 3. Histograms showing the distribution of PAV (%) in coronary arteries supplying non-ischemic (A, B and C; histogram bars in blue) and ischemic (D, E and F; histogram bars in red) myocardial territories for LAD (A and D), LCx (B and E) and RCA (C and F).

Table 4. **Comparison of AI-QCT characteristics of different coronary arteries supplying ischemic myocardial territories**

	LAD Ischemic	LCX Ischemic	RCA Ischemic	P-value	P-value LAD vs LCX	P-value LAD vs RCA	P-value LCX vs RCA
Vessel volume, mm^3	1216 [954-1501]	963 [638-1291]	1210 [930-1591]	<.001	<.001	1.000	<.001
Lumen volume, mm^3	927 [744-1142]	790 [497-1099]	985 [685-1303]	<.001	.001	.749	<.001
Remodeling index	1.4 [1.3-1.6]	1.4 [1.2-1.5]	1.3 [1.2-1.5]	<.001	<.001	<.001	.530
Diameter stenosis, %	55 [39-71]	31 [18-50]	45 [24-66]	<.001	<.001	.001	.001
Area stenosis, %	82 [62-92]	52 [32-75]	69 [40-89]	<.001	<.001	<.001	<.001
Total plaque volume, mm^3	241 [148-380]	125 [50-221]	176 [75-348]	<.001	<.001	<.001	<.001
NCPV, mm^3	128 [77-200]	67 [34-112]	106 [44-200]	<.001	<.001	.031	<.001
CPV, mm^3	89 [31-197]	38 [10-104]	44 [8-137]	<.001	<.001	<.001	.922
PAV, %	21 [13-31]	14 [6-24]	16 [7-27]	<.001	<.001	<.001	.623
Percent NCPV, %	11 [7-16]	7 [4-13]	9 [6-16]	<.001	<.001	.011	.134
Percent CPV, %	8 [3-16]	4 [1-10]	4 [1-11]	<.001	<.001	<.001	1.000
Low attenuation plaque, n(%)	125 (45)	45 (21)	73 (34)	<.001	<.001	.079	.009

Values are n (%) or median [interquartile range].
AI-QCT, artificial intelligence-guided quantitative computed tomography; *LAD*, left descending artery; *LCX*, left circumflex artery; *RCA*, right coronary artery; *NCPV*, non-calcified plaque volume; *CPV*, calcified plaque volume. For pairwise comparisons, *P*-values were adjusted using the Dunn's correction for multiple tests or the Bonferroni correction to control for multiple comparisons.

index, and all measures of plaque burden were significantly associated with ischemia in all vessels in univariable analyses. In multivariable analysis 1, when PAV was included as a measure of total plaque burden, stenosis severity and PAV were both associated with ischemia in all three main coronary arteries, whereas remodeling index was not. In multivariable analysis 2, when percent NCPV and CPV where included in the analysis (instead of total plaque), stenosis degree and percent NCPV were associated with ischemia in all three vessels. In addition, percent CPV was independently associated with ischemia in the RCA, but not in the LAD or LCX. Presence of low-attenuation plaque was not associated with ischemia in any of the vessels in the multivariable analyses.

For each coronary artery, a receiver operating characteristic (ROC) curve for prediction of myocardial ischemia based on vessel diameter stenosis and the estimated probability of ischemia as a function of diameter stenosis is

Table 5. Univariable and multivariable logistic regression analysis to identify AI-QCT parameters associated with the presence of myocardial ischemia. Multivariable regression analysis 1 includes percentages of total plaque volume (PAV%) and multivariable regression analysis 2 includes percentages of subcomponents of plaque volumes (NCPV% and CPV%)

	Univariable analysis			Multivariable analysis 1				Multivariable analysis 2			
	Odds ratio	95% CI	P-value	Odds ratio	95% CI	P-value	VIF	Odds ratio	95% CI	P-value	VIF
LAD											
Remodeling index	1.32	1.22-1.43	**<.001**	1.09	1.00-1.20	.060	1.45	1.08	.99-1.19	.097	1.50
Diameter stenosis, %	1.04	1.03-1.05	**<.001**	1.03	1.02-1.04	**<.001**	1.84	1.02	1.01-1.03	**<.001**	1.98
Area stenosis, %	1.04	1.03-1.04	**<.001**	–	–	–	–	–	–	–	–
Total plaque volume, mm^3	1.004	1.003-1.005	**<.001**	–	–	–	–	–	–	–	–
NCPV, mm^3	1.007	1.006-1.009	**<.001**	–	–	–	–	–	–	–	–
CPV, mm^3	1.004	1.003-1.006	**<.001**	–	–	–	–	–	–	–	–
Percent atheroma volume, %	1.08	1.06-1.09	**<.001**	1.03	1.01-1.05	**<.001**	2.14	–	–	–	–
Percent NCPV, %	1.16	1.12-1.19	**<.001**	–	–	–	–	1.07	1.03-1.11	**.001**	2.19
Percent CPV, %	1.07	1.05-1.09	**<.001**	–	–	–	–	1.02	1.00-1.05	.052	1.47
Presence of low attenuation plaque	2.17	2.17-4.04	**<.001**	1.38	.97-1.98	.074	1.23	1.22	.83-1.79	.308	1.40
LCX											
Remodeling index	1.24	1.15-1.33	**<.001**	1.00	.91-1.10	.982	1.74	1.00	.90-1.10	.942	1.75
Diameter stenosis, %	1.04	1.03-1.05	**<.001**	1.03	1.02-1.04	**<.001**	1.97	1.02	1.01-1.04	**<.001**	2.07
Area stenosis, %	1.03	1.02-1.03	**<.001**	–	–	–	–	–	–	–	–
Total plaque volume, mm^3	1.01	1.003-1.006	**<.001**	–	–	–	–	–	–	–	–
NCPV, mm^3	1.01	1.006-1.011	**<.001**	–	–	–	–	–	–	–	–
CPV, mm^3	1.01	1.005-1.010	**<.001**	–	–	–	–	–	–	–	–
Percent atheroma volume, %	1.07	1.05-1.08	**<.001**	1.03	1.01-1.06	**.003**	2.36	–	–	–	–
Percent NCPV, %	1.13	1.09-1.16	**<.001**	–	–	–	–	1.05	1.01-1.10	**.014**	2.34
Percent CPV, %	1.08	1.06-1.11	**<.001**	–	–	–	–	1.02	1.00-1.05	.112	1.62
Presence of low attenuation plaque	1.85	1.23-2.77	**.003**	.90	.57-1.43	.657	1.14	.85	.53-1.37	.501	1.20
RCA											
Remodeling index	1.37	1.25-1.50	**<.001**	.91	.80-1.04	.180	1.95	.91	.80-1.04	.178	1.97
Diameter stenosis, %	1.04	1.03-1.05	**<.001**	1.03	1.02-1.03	**<.001**	2.04	1.02	1.02-1.03	**<.001**	2.21
Area stenosis, %	1.03	1.02-1.04	**<.001**	–	–	–	–	–	–	–	–
Total plaque volume, mm^3	1.004	1.003-1.005	**<.001**	–	–	–	–	–	–	–	–
NCPV, mm^3	1.01	1.004-1.008	**<.001**	–	–	–	–	–	–	–	–
CPV, mm^3	1.01	1.004-1.007	**<.001**	–	–	–	–	–	–	–	–
Percent atheroma volume, %	1.08	1.06-1.10	**<.001**	1.05	1.03-1.07	**<.001**	2.46	–	–	–	–
Percent NCPV, %	1.14	1.11-1.17	**<.001**	–	–	–	–	1.05	1.01-1.10	**.017**	2.87
Percent CPV, %	1.10	1.07-1.13	**<.001**	–	–	–	–	1.05	1.02-1.08	**.001**	1.49
Presence of low attenuation plaque	3.21	2.21-4.67	**<.001**	1.36	.87-2.13	.179	1.26	1.35	.84-2.17	.218	1.40

AI-QCT, artificial intelligence-guided quantitative computed tomography; *CI*, confidence interval; *VIF*, variance inflation factor; *LAD*, left descending artery; *LCX*, left circumflex artery; *RCA*, right coronary artery; *NCPV*, non-calcified plaque volume; *CPV*, calcified plaque volume.

shown in Figure 4. The performance of diameter stenosis for prediction of ischemia did not differ between the vessels (AUC = .73 for LAD, AUC = .70 for LCX, and AUC = .74 for RCA; ns between all). The modeled diameter stenosis degree (95% CI) to have 50% probability of ischemia was 63% (58%-68%) for the LAD, 57% (50%-66%) for the LCX, and 59% (53%-66%) for the RCA (ns between all).

Figure 5 shows ROC curves for prediction of myocardial ischemia based on vessel PAV and the estimated probability of ischemia as a function of PAV from logistic regression. The performance of PAV in prediction of ischemia did not differ between the vessels (AUC = .72 for the LAD, AUC = .70 for the LCX, and AUC = .73 for the RCA; ns between all). The modeled PAV (95% CI) to have 50% probability of ischemia was 26.5% (24.0%-29.6%) for the LAD, 28.5% (24.7%-34.2%) for the LCX and 24.0% (21.1%-27.7%) for the RCA (ns between all).

Supplemental Table 1 shows a comparison of the performance of vessel diameter stenosis and the plaque burden measures in prediction of myocardial ischemia in the three main coronary arteries. In terms of AUC, adding PAV on top of

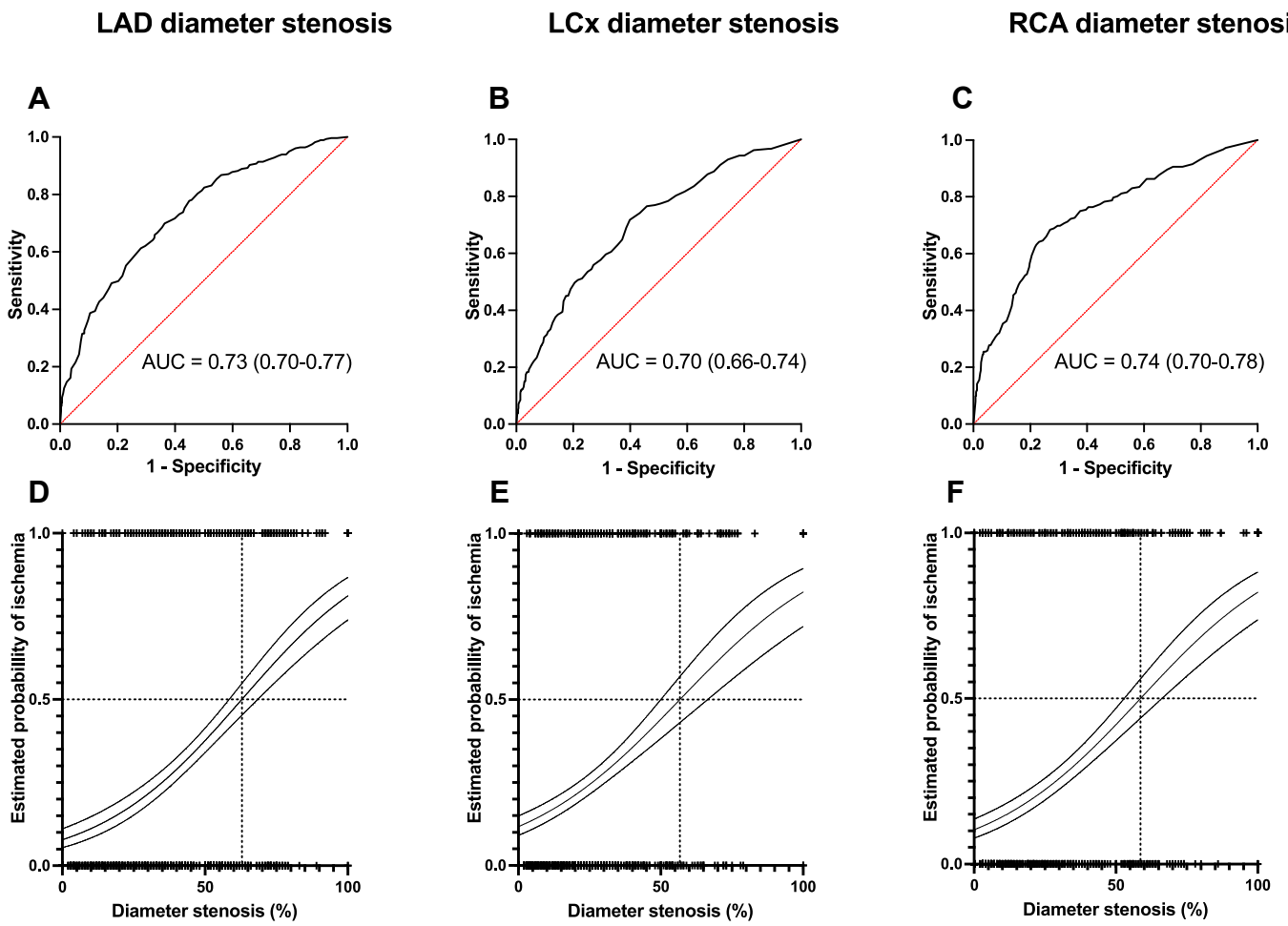

|Figure 4. Receiver operating characteristic (ROC) curves for discrimination for myocardial ischemia based on vessel diameter stenosis in LAD (panel A), LCX (panel B) and RCA (panel C). The predicted probability of ischemia (with dashed lines for 95% CI) as a function of diameter stenosis is shown in panels D, E, and f for LAD, LCX, and RCA, respectively, derived from univariable binary logistic regression analyses. The dotted lines in panels D, E, and F show the vessel diameter stenosis degree where the probability of ischemia is 50%: LAD diameter stenosis (95% CI) 63 % (58%-68%); LCX diameter stenosis 57% (50%-66%), and RCA diameter stenosis 59% (53%-66%). LAD, left anterior descending coronary artery, LCX, left circumflex coronary artery, RCA, right coronary artery.

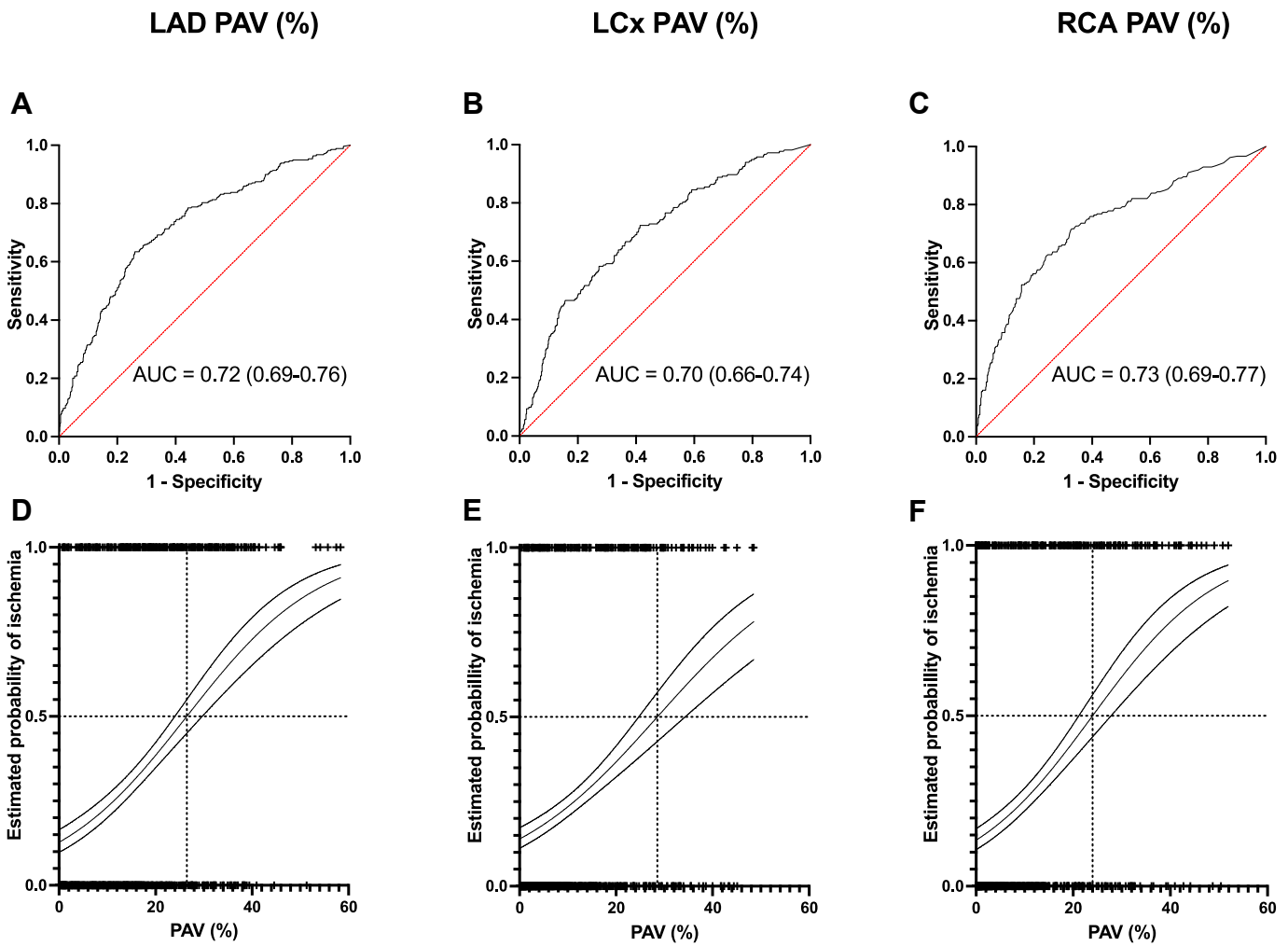

Figure 5. Receiver operating characteristic (ROC) curves for discrimination for myocardial ischemia based on percent atheroma volume (PAV) in LAD (panel A), LCX (panel B), and RCA (panel C). The predicted probability of ischemia (with dashed lines for 95% CI) as a function of PAV is shown in panels D, E, and F for LAD, LCX, and RCA, respectively, derived from univariable binary logistic regression analyses. The dotted lines in panels D, E, and F show the vessel PAV where the probability of ischemia is 50%: LAD PAV (95% CI) 26.5% (24.0%-29.6%), LCX PAV 28.5% (24.7%-34.2 %) and RCA PAV 24.0% (21.1%-27.7 %). LAD, left anterior descending coronary artery, LCX, left circumflex coronary artery, RCA, right coronary artery.

diameter stenosis improved the discrimination for ischemia in all the main coronary arteries (for the LAD .73 [.70-.77] vs .75 [.72-.79], $P = .005$; for the LCX .70 [.66-.74] vs .72 [.68-.76], $P = .040$; and for the RCA .74 [.70-.78] vs .76 [.72-.80], $P = .006$).

Adding NCPV or CPV on top of diameter stenosis improved the discrimination for ischemia in the LAD and RCA, but not in the LCX (see Supplemental Table 1 for details).

Supplemental Table 2 shows that there were no significant differences between the three coronary arteries in the performance of the diameter stenosis or plaque burden measures to predict myocardial ischemia (not significant between all).

DISCUSSION

In this cohort of symptomatic patients undergoing *coronary* CTA and PET MPI for suspected CAD, we assessed and compared the atherosclerotic burden and phenotype of the major epicardial coronary arteries supplying ischemic myocardial territories.

The main findings of this study are:

1) The stenosis severity and atherosclerotic burden are higher in the LAD as compared to the other coronary arteries, even when normalized for vessel size. This is also true for vessels supplying ischemic territories, where the severity of luminal narrowing is clearly lower in the LCX, followed by the RCA, as compared to the LAD.
2) As expected, the main epicardial coronary arteries supplying ischemic myocardial territories have more advanced atherosclerosis than those supplying nonischemic territories. However, there are still many vessels supplying ischemic territories with relatively low stenosis degree and plaque burden; this was especially true for the LCX and the RCA.
3) Both coronary artery luminal narrowing and plaque burden, the latter mainly driven by noncalcified plaque, are independent predictors of myocardial ischemia, without major differences between the three vessels.

The strength of the current study is the detailed, quantitative plaque analysis on a vessel level that complements the previous paper by Bax et al. [6] by now adding objective quantitative ischemia assessment by PET MPI. Similar to the findings by Bax et al., we found that atherosclerotic burden significantly differs between the coronary arteries, with the highest degree of stenosis and plaque burden observed in the LAD. In contrast, plaque burden in the LCX and RCA was comparable with each other when normalized to the vessel volume in the current study. However, Bax et al. reported more calcified plaque in the LCX as compared to the LAD and RCA, whereas low-density plaque was more prevalent in the LAD and RCA [6]. In our cohort, however, all the different plaque types were most prevalent in the LAD. These different findings between the studies could be possibly be explained by differences in patient selection; patients included in our study might have more advanced CAD because only patients with suspected obstructive stenosis on CTA were referred to downstream ischemia testing by PET.

In the present study, the LAD demonstrated a higher plaque burden and greater degree of stenosis compared to the other coronary vessels, and this was true among both ischemic and nonischemic myocardial territories. This likely accounts for the absence of significant vessel-specific differences in the association between atherosclerotic plaque characteristics and myocardial ischemia observed in the logistic regression analyses, despite regional variation in plaque features. This is illustrated by the sigmoid curves (Figures 4 and 5) showing that a comparable degree of stenosis (ranging from 57%-63%) or plaque burden (PAV ranging from 24.0%-28.5%) for different vessels is needed to have 50% probability of vessel-specific ischemia. Interestingly, based on our comparison of AUCs (Supplemental Table 1), it seems that PAV performs equally to diameter stenosis in discrimination for ischemia, and this was true for all the main coronary arteries. More surprising is the observation that many patients had relatively low degree of stenosis and low PAV in the LCX and the RCA, both in vessels supplying ischemic as well as nonischemic territories. It is well known that the vessel stenosis degree has a relatively low predictive value for ischemia [20–22]. Previous evidence suggests [23] that in single-vessel obstructive CAD, nonobstructive "remote" coronary arteries may also have impaired myocardial perfusion. Moreover, a prior study from our center [24] demonstrated that coronary microvascular dysfunction often coexists with obstructive CAD. Therefore, coronary microvascular dysfunction or otherwise impaired vasodilating capability might partly explain our observations of myocardial ischemia in coronary arteries with relatively low stenosis degree.

Given that the LAD is more commonly affected by atherosclerotic disease [6], the higher plaque burden and stenosis observed in the LAD likely reflects both the natural history of CAD and the clinical referral process for further imaging. This may have contributed to the greater representation of LAD disease in our cohort and should be considered when interpreting vessel-level

comparisons. While several possible explanations have been proposed for the differences in the development of atherosclerosis between the main coronary arteries (e.g. local hemodynamic forces and differences in wall shear stress [25,26]) the relationship between coronary artery stenosis degree and myocardial ischemia remains imperfectly understood. More accurate measures of stenosis severity, e.g. minimal lumen diameter and area, have not been able to strengthen the relation between stenosis and ischemia [27]. Apparently, other geometric variables besides lumen narrowing have impact on coronary blood flow, e.g. plaque length and volume [28,29]; however, this was not tested in the current work. More recently, plaque burden, plaque characteristics, and positive remodeling have been reported to be predictive of ischemia [3]. However, none of these features are able to explain our findings of ischemia with lower stenosis degree in the LCX and the RCA regions as compared to the LAD. Other pathophysiological mechanisms for ischemia have been proposed. Inflammation, local endothelial dysfunction, and altered shear stress patterns could possibly explain ischemia in the early stage of atherosclerosis [3], but if those mechanisms differ between the main coronary arteries remains to be studied.

If applying the standard criterion for significant luminal narrowing (i.e. 50%), we would expect a low sensitivity for detection of ischemia, especially in the LCX and RCA (see Figure 2). Choosing an optimal cut-off value for diameter stenosis or PAV to predict myocardial ischemia seems not easy, as there is a significant overlap in the stenosis degree and PAV in vessels supplying ischemic and nonischemic regions. This is also reflected by the relatively flat shape of the ROC curves shown in our study (Figures 4 and 5). Combining quantitative measures of stenosis degree and plaque could possibly improve the diagnostic accuracy. In an earlier study, we reported that the addition of AI-QCT quantitative measures of PAV and NCPV to the degree of stenosis improved the detection of ischemic CAD on a patient level [10].

In a selected cohort of 192 patients with at least one vessel with $\geq$50% diameter stenosis, Belmonte et al. investigated vessel-specific morphological plaque features as predictors of ischemia as defined by positive invasive fractional flow reserve (FFR) and reported that the combination of coronary artery stenosis severity and vessel-specific morphological plaque features from coronary CTA significantly increased the predictive performance for vessel-specific ischemia compared to diameter stenosis alone [30]. Similar to Belmonte et al. we noted that the coronary plaque characteristics, in addition to luminal narrowing, provide incremental predictive value for ischemia in all main vessels. In our study stenosis degree, PAV, and percent NCPV were independent predictors of ischemia in all three main coronary arteries. Adding PAV on top of diameter stenosis improved the discrimination for ischemia in all the main coronary arteries, whereas adding NCPV on top of diameter stenosis improved the discrimination for ischemia in the LAD and RCA, but not in the LCX. Calcified plaque measures seem to perform less well as predictor of ischemia both at a per-patient level (previous study [10]) and at a per-vessel level (current study and Belmonte et al. [30]).

Even though our cohort was selected based on the presence of at least one visually suspected obstructive stenosis on CTA, our analysis still covers a wide range of stenosis severities, including also nonobstructive vessels. This can be seen as a strength of our study, e.g. as compared with the study by Belmonte et al., where functional assessment (i.e. invasive FFR) was restricted to obstructive vessels, whereas our use of PET allows for assessment of ischemia in all vessels. This broader coverage (i.e. less selection) enables a more comprehensive evaluation of the relationship between plaque features and perfusion, including vessels that might otherwise be overlooked.

Driessen et al. also evaluated the association between quantitative plaque measures and myocardial perfusion [31] on a vessel level, although they did not compare the findings between the different coronary arteries. Similar to our findings, they reported that NCPVs were associated with impaired MBF independently of stenosis severity. Driessen et al. reported that positive remodeling also was an independent predictor of ischemia; however, in the current study we could not reproduce this as a vessel-specific determinant of ischemia.

Our findings are in line with several earlier studies showing that coronary plaque parameters, such as total plaque volume and percent atheroma volume, are predictors of myocardial ischemia [31–34]. By integrating several coronary atherosclerosis and vascular morphology characteristics, a newly developed AI-QCT$_{\text{ISCHEMIA}}$ algorithm was able to diagnose coronary ischemia accurately both at a per-patient and a per-vessel level [35].

Limitations

This was a single-center, observational study with the limitations of a retrospective setting. The study population represents symptomatic

patients, of whom those with at least one visually obstructive stenosis on coronary CTA were referred for downstream PET perfusion imaging [1], aiming at identification of hemodynamically significant (ischemic) epicardial CAD rather than coronary microvascular dysfunction. A potential limitation of our study is the presence of referral bias, as patients were selected for PET MPI based on findings from coronary CTA, often in the context of suspected or visually identified obstructive CAD. As a result, the interaction between nonobstructive CAD and myocardial ischemia could not be fully assessed based on our study. Despite this selection, the patients in the study had a broad range of coronary artery stenosis degrees according to the AI-QCT results.

A limitation of this study is the use of standard coronary artery territories for assigning myocardial perfusion defects, although we adjusted for coronary dominance. Detailed vessel-to-territory matching based on hybrid or fusion imaging was not feasible, as such data were not available. This may have led to misassignment of ischemic regions, particularly in the LCX and RCA territories [36]. Although patients with known prior MI, PCI, or CABG were not included, the presence of unrecognized previous MI cannot be entirely excluded and may have contributed to reduced stress perfusion in some myocardial regions, including areas with total occlusions. No information on vessel territory size/myocardial mass supplied was available.

We classified myocardial territories as ischemic or nonischemic based on the previously validated binary cut-off of 2.3 mL $min^{-1}g^{-1}$ [37] but did not account for the extent or severity of ischemic burden. Future studies should explore the relationship between plaque characteristics and ischemic burden, as this may offer deeper functional insights into the impact of plaque features. Incorporating measures of ischemic burden could help clarify the clinical relevance of the observed anatomical differences. Another limitation is the potential discrepancy between visual CTA assessment, broadly used for clinical decision-making and the AI-QCT-derived measurements used in our study. However, a recent study suggested that AI-QCT can outperform clinical visual CTA reading when benchmarked against invasive quantitative coronary angiography [13]. Moreover, due to the lack of detailed visual grading, we were unable to reclassify patients by, e.g. visual CAD-RADS categories. Importantly, our models included stenosis degree as a continuous variable, preserving its statistical power and therefore reducing the risk of artificially inflating the importance of other plaque features. However, in a sensitivity analysis using the visual classification of coronary stenosis (obstructive vs nonobstructive) instead of percent diameter stenosis from AI-QCT, the plaque parameters remained independently associated with ischemia (Supplemental Table 3).

New knowledge gained and clinical implications

Among coronary arteries supplying ischemic myocardial territories, the LAD shows more advanced atherosclerosis, whereas many LCX and RCA vessels have relatively low degree of stenosis and low plaque burden. Therefore, if applying the standard criterion for significant luminal narrowing (50%), we would expect a low sensitivity for detection of ischemia, especially in the LCX and RCA. Plaque burden seems to perform equally to diameter stenosis degree in discrimination for ischemia.

CONCLUSIONS

In all the three main coronary arteries, both luminal narrowing and plaque burden, mainly driven by noncalcified plaque, are independent predictors of myocardial ischemia. The degree of stenosis and atherosclerotic burden are significantly higher in LAD as compared to the LCX and RCA, both in epicardial coronary arteries supplying nonischemic or ischemic myocardial territories. However, many vessels supplying ischemic territories have relatively low stenosis degree and plaque burden, especially in the LCX and RCA, limiting the ability of diameter stenosis and PAV to predict myocardial ischemia.

FUNDING AND SUPPORT

The study was funded by the Finnish Foundation for Cardiovascular Research, Finnish State Research Funding [VTR 13403], and the Research Council of Finland. Dr Bär was supported by the Swiss National Science Foundation [P500PM_210788], Dr Kero by the Swedish Heart Association and the University of Turku, Finland; and from an unrestricted grant provided by Cleerly Inc. Cleerly Inc. performed the image analysis without costs.

DISCLOSURES

The authors declare the following financial interests/personal relationships which may be considered as potential competing interests: Tanja Kero reports financial support was provided by the Swedish Heart and Lung Association. Tanja Kero reports financial support was provided by University of Turku. Sarah Bar reports financial support was provided by the Finnish Foundation for Cardiovascular Research. Sarah Bar reports financial support was provided by the

Swiss National Science Foundation. Sarah Bar reports a relationship with Cleerly Inc. that includes speaking and lecture fees. Sarah Bar reports a relationship with Sanofi that includes travel reimbursement. Juhani Knuuti reports a relationship with GE Healthcare that includes consulting or advisory. Juhani Knuuti reports a relationship with Synectic that includes consulting or advisory. Juhani Knuuti reports a relationship with Bayer that includes speaking and lecture fees. Juhani Knuuti reports a relationship with Lundbeck that includes speaking and lecture fees. Juhani Knuuti reports a relationship with Boehringer Ingelheim that includes speaking and lecture fees. Juhani Knuuti reports a relationship with Pfizer that includes speaking and lecture fees. Juhani Knuuti reports a relationship with Siemens that includes speaking and lecture fees. Antti Saraste reports a relationship with Astra Zeneca that includes consulting or advisory. Antti Saraste reports a relationship with Pfizer that includes consulting or advisory. Antti Saraste reports a relationship with Abbott that includes speaking and lecture fees. Antti Saraste reports a relationship with Astra Zeneca that includes speaking and lecture fees. Antti Saraste reports a relationship with Janssen that includes speaking and lecture fees. Antti Saraste reports a relationship with Novartis that includes speaking and lecture fees. Antti Saraste reports a relationship with Pfizer that includes speaking and lecture fees. Jeroen Bax reports a relationship with Abbott that includes speaking and lecture fees. If there are other authors, they declare that they have no known competing financial interests or personal relationships that could have appeared to influence the work reported in this paper.

APPENDIX A. SUPPLEMENTARY DATA

Supplementary data to this article can be found online at https://doi.org/10.1016/j.nuclcard.2025.102470.

REFERENCES

[1] Vrints C, Andreotti F, Koskinas KC, Rossello X, Adamo M, Ainslie J, et al. 2024 ESC guidelines for the management of chronic coronary syndromes. Eur Heart J 2024;45(36):3415–3537.

[2] Nielsen CG, Laut KG, Jensen LO, Ravkilde J, Terkelsen CJ, Kristensen SD. Patient delay in patients with ST-elevation myocardial infarction: time patterns and predictors for a prolonged delay. Eur Heart J Acute Cardiovasc Care 2017;6:583–591.

[3] Ahmadi A, Senoner T, Correa A, Feuchtner G, Narula J. How atherosclerosis defines ischemia: atherosclerosis quantification and characterization as a method for determining ischemia. J Cardiovasc Comput Tomogr 2020;14:394–399.

[4] Lin A, van Diemen PA, Motwani M, McElhinney P, Otaki Y, Han D, et al. Machine learning from quantitative coronary computed tomography angiography predicts fractional flow reserve-defined ischemia and impaired myocardial blood flow. Circ Cardiovasc Imag 2022;15:e014369.

[5] Stuijfzand WJ, van Rosendael AR, Lin FY, Chang HJ, van den Hoogen IJ, Gianni U, et al. Stress myocardial perfusion imaging vs coronary computed tomographic angiography for diagnosis of invasive vessel-specific coronary physiology: predictive modeling results from the computed tomographic evaluation of atherosclerotic determinants of myocardial ischemia (CREDENCE) trial. JAMA Cardiol 2020;5:1338–1348.

[6] Bax AM, van Rosendael AR, Ma X, van den Hoogen IJ, Gianni U, Tantawy SW, et al. Comparative differences in the atherosclerotic disease burden between the epicardial coronary arteries: quantitative plaque analysis on coronary computed tomography angiography. Eur Heart J Cardiovasc Imag 2021;22:322–330.

[7] Singh V, Choi AD, Leipsic J, Aghayev A, Earls JP, Blanke P, et al. Use of cardiac CT amidst the COVID-19 pandemic and beyond: north American perspective. J Cardiovasc Comput Tomogr 2021;15:16–26.

[8] Griffin WF, Choi AD, Riess JS, Marques H, Chang HJ, Choi JH, et al. AI evaluation of stenosis on coronary CTA, comparison with quantitative coronary angiography and fractional flow reserve: a CREDENCE trial substudy. JACC Cardiovascular Imag 2023;16:193–205.

[9] Lipkin I, Telluri A, Kim Y, Sidahmed A, Krepp JM, Choi BG, et al. Coronary CTA with AI-QCT interpretation: Comparison with myocardial perfusion imaging for detection of obstructive stenosis using invasive angiography as reference standard. AJR American J Roentgenol 2022;219:407–419.

[10] Kero T, Bär S, Saraste A, Klén R, Bax JJ, Knuuti J, Maaniitty T. Plaque burden improves the detection of ischemic CAD over stenosis from coronary computed tomography angiography. Int J Cardiovasc Imag 2025;41(6):1131–1140.

[11] Kajander S, Joutsiniemi E, Saraste M, Pietila M, Ukkonen H, Saraste A, et al. Cardiac positron emission tomography/computed tomography imaging accurately detects anatomically and functionally significant coronary artery disease. Circulation 2010;122:603–613.

[12] Maaniitty T, Stenstrom I, Bax JJ, Uusitalo V, Ukkonen H, Kajander S, et al. Prognostic value of coronary CT angiography with selective PET perfusion imaging in coronary artery disease. JACC Cardiovascular Imag 2017;10:1361–1370.

[13] Bernardo R, Nurmohamed NS, Bom MJ, Jukema R, de Winter RW, Sprengers R, et al. Diagnostic accuracy in coronary CT angiography analysis: artificial intelligence versus human assessment. Open Heart 2025;12.

[14] Shaw LJ, Blankstein R, Bax JJ, Ferencik M, Bittencourt MS, Min JK, et al. Society of cardiovascular computed tomography/North American society of cardiovascular imaging - expert consensus document on coronary CT imaging of atherosclerotic plaque. Journal of cardiovascular computed tomography 2021;15:93–109.

[15] Cerqueira MD, Weissman NJ, Dilsizian V, Jacobs AK, Kaul S, Laskey WK, et al. Standardized myocardial segmentation and nomenclature for tomographic imaging of the heart. A statement for healthcare professionals from the cardiac imaging committee of the council on clinical cardiology of the American heart association. Circulation 2002;105:539–542.

[16] Danad I, Uusitalo V, Kero T, Saraste A, Raijmakers PG, Lammertsma AA, et al. Quantitative assessment of myocardial perfusion in the detection of significant

coronary artery disease: cutoff values and diagnostic accuracy of quantitative [(15)O]H2O PET imaging. J Am Coll Cardiol 2014;64:1464–1475.

[17] DeLong ER, DeLong DM, Clarke-Pearson DL. Comparing the areas under two or more correlated receiver operating characteristic curves: a nonparametric approach. Biometrics 1988;44:837–845.

[18] Hanley JA, McNeil BJ. The meaning and use of the area under a receiver operating characteristic (ROC) curve. Radiology 1982;143:29–36.

[19] Hanley JA, McNeil BJ. A method of comparing the areas under receiver operating characteristic curves derived from the same cases. Radiology 1983;148:839–843.

[20] Gould KL, Johnson NP, Bateman TM, Beanlands RS, Bengel FM, Bober R, et al. Anatomic versus physiologic assessment of coronary artery disease. Role of coronary flow reserve, fractional flow reserve, and positron emission tomography imaging in revascularization decision-making. J Am Coll Cardiol 2013;62:1639–1653.

[21] Meijboom WB, Van Mieghem CA, van Pelt N, Weustink A, Pugliese F, Mollet NR, et al. Comprehensive assessment of coronary artery stenoses: computed tomography coronary angiography versus conventional coronary angiography and correlation with fractional flow reserve in patients with stable angina. J Am Coll Cardiol 2008;52:636–643.

[22] Tonino PA, Fearon WF, De Bruyne B, Oldroyd KG, Leesar MA, Ver Lee PN, et al. Angiographic versus functional severity of coronary artery stenoses in the FAME study fractional flow reserve versus angiography in multivessel evaluation. J Am Coll Cardiol 2010;55:2816–2821.

[23] Sambuceti G, Marzullo P, Giorgetti A, Neglia D, Marzilli M, Salvadori P, et al. Global alteration in perfusion response to increasing oxygen consumption in patients with single-vessel coronary artery disease. Circulation 1994;90:1696–1705.

[24] Stenstrom I, Maaniitty T, Uusitalo V, Pietila M, Ukkonen H, Kajander S, et al. Frequency and angiographic characteristics of coronary microvascular dysfunction in stable angina: a hybrid imaging study. Eur Heart J Cardiovasc Imag 2017;18:1206–1213.

[25] Malek AM, Jiang L, Lee I, Sessa WC, Izumo S, Alper SL. Induction of nitric oxide synthase mRNA by shear stress requires intracellular calcium and G-protein signals and is modulated by PI 3 kinase. Biochem Biophys Res Commun 1999;254:231–242.

[26] Slager CJ, Wentzel JJ, Gijsen FJ, Schuurbiers JC, van der Wal AC, van der Steen AF, et al. The role of shear stress in the generation of rupture-prone vulnerable plaques. Nat Clin Pract Cardiovasc Med 2005;2:401–407.

[27] Johnson NP, Kirkeeide RL, Gould KL. Coronary anatomy to predict physiology: fundamental limits. Circulation Cardiovascular Imag 2013;6:817–832.

[28] Kimball BP, Dafopoulos N, LiPreti V. Comparative evaluation of coronary stenoses using fluid dynamic equations and standard quantitative coronary arteriography. Am J Cardiol 1989;64:6–10.

[29] Takayama T, Hodgson JM. Prediction of the physiologic severity of coronary lesions using 3D IVUS: validation by direct coronary pressure measurements. Cathet Cardiovasc Interv : official J Society for Cardiac Angiography & Interventions 2001;53:48–55.

[30] Belmonte M, Paolisso P, Gallinoro E, Bertolone DT, Leone A, Esposito G, et al. Improved diagnostic accuracy of vessel-specific myocardial ischemia by coronary computed tomography angiography (CCTA). J Cardiovasc Comput Tomogr 2025;19(1):17–25.

[31] Driessen RS, Stuijfzand WJ, Raijmakers PG, Danad I, Min JK, Leipsic JA, et al. Effect of plaque burden and morphology on myocardial blood flow and fractional flow reserve. J Am Coll Cardiol 2018;71:499–509.

[32] Ahmadi A, Leipsic J, Ovrehus KA, Gaur S, Bagiella E, Ko B, et al. Lesion-specific and vessel-related determinants of fractional flow reserve beyond coronary artery stenosis. JACC Cardiovascular Imag 2018;11:521–530.

[33] Gaur S, Ovrehus KA, Dey D, Leipsic J, Botker HE, Jensen JM, et al. Coronary plaque quantification and fractional flow reserve by coronary computed tomography angiography identify ischaemia-causing lesions. Eur Heart J 2016;37:1220–1227.

[34] Park HB, Heo R, B OH, Cho I, Gransar H, Nakazato R, et al. Atherosclerotic plaque characteristics by CT angiography identify coronary lesions that cause ischemia: a direct comparison to fractional flow reserve. JACC Cardiovascular Imag 2015;8:1–10.

[35] Nurmohamed NS, Danad I, Jukema RA, de Winter RW, de Groot RJ, Driessen RS, et al. Development and validation of a quantitative coronary CT angiography model for diagnosis of vessel-specific coronary ischemia. JACC Cardiovascular Imag 2024;17:894–906.

[36] Liga R, Vontobel J, Rovai D, Marinelli M, Caselli C, Pietila M, et al. Multicentre multi-device hybrid imaging study of coronary artery disease: results from the EValuation of INtegrated cardiac imaging for the detection and characterization of ischaemic heart disease (EVINCI) hybrid imaging population. Eur Heart J Cardiovasc Imag 2016;17:951–960.

[37] Danad I, Raijmakers PG, Driessen RS, Leipsic J, Raju R, Naoum C, et al. Comparison of coronary CT angiography, SPECT, PET, and hybrid imaging for diagnosis of ischemic heart disease determined by fractional flow reserve. JAMA Cardiol 2017;2(10):1100–1107.